

Article

Rapid Fleet Condition Analysis through Correlating Basic Vehicle Tracking Data with Engine Oil FT-IR Spectra

András Lajos Nagy ^{1,*} , Adam Agocs ², Bettina Ronai ², Péter Raffai ³, Jan Rohde-Brandenburger ^{1,3}, Charlotte Besser ² and Nicole Dörr ²

¹ Department of Internal Combustion Engines and Propulsion Technology, Széchenyi István University, Egyetem tér 1, 9026 Győr, Hungary; jan.rohde-brandenburger@audi.hu

² AC2T research GmbH, Viktor-Kaplan-Straße 2C, 2700 Wiener Neustadt, Austria; adam.agocs@ac2t.at (A.A.); bettina.ronai@ac2t.at (B.R.); charlotte.besser@ac2t.at (C.B.); Nicole.Doerr@ac2t.at (N.D.)

³ Audi Hungaria Zrt, Audi Hungária út 1, 9027 Győr, Hungary; peter.raffai@audi.hu

* Correspondence: nagy.andras1@sze.hu

Abstract: Engine oil condition and tribological performance are strongly interrelated. Accordingly, oil condition monitoring is common in various applications. This is especially important, as oil condition depends on the fueling and utilization profile of an internal combustion engine. Common practice involves the measurement of various parameters, such as the total acid number and total base number, oxidation, nitration, viscosity, and elemental composition; thus, it can be time-consuming and resource-intensive. This study provides a methodology for rapid analysis for large vehicle fleets or sample sizes, using only Fourier-transformed infrared spectroscopy and the subsequent multivariate data analysis offers a rapid alternative to commonly available methods. The described method provides a rapid, cost-efficient, and intuitive approach to uncovering differences in the oil condition. Furthermore, understanding the underlying reasons in engine construction and the resulting chemical degradation is also possible.

Keywords: lubricants; tribology; wear; measurements; fuel dilution



Citation: Nagy, A.L.; Agocs, A.; Ronai, B.; Raffai, P.; Rohde-Brandenburger, J.; Besser, C.; Dörr, N. Rapid Fleet Condition Analysis through Correlating Basic Vehicle Tracking Data with Engine Oil FT-IR Spectra. *Lubricants* **2021**, *9*, 114. <https://doi.org/10.3390/lubricants9120114>

Received: 27 September 2021
Accepted: 18 November 2021
Published: 24 November 2021

Publisher's Note: MDPI stays neutral with regard to jurisdictional claims in published maps and institutional affiliations.



Copyright: © 2021 by the authors. Licensee MDPI, Basel, Switzerland. This article is an open access article distributed under the terms and conditions of the Creative Commons Attribution (CC BY) license (<https://creativecommons.org/licenses/by/4.0/>).

1. Introduction

The European Union has set a clear goal in decarbonizing the transportation sector [1]. Member states are establishing their timeline for limiting new vehicle sales to zero-emission solutions for passenger cars [2], and the automotive industry is responding by introducing purely electric options [3–5] and investing in fuel-cell [6,7], battery [8,9], and hydrogen technologies [10–12]. Still, internal combustion engines (ICEs) are predominant amongst drivetrain technologies in present days. The European Automobile Manufacturers' Association (ACEA) reports [13] that in 2020, newly registered vehicles were still primarily propelled by petrol (47.5%) and diesel (28.0%), followed by hybrid electric vehicles (11.9%) and plug-in hybrid electric vehicles (5.4%). Battery electric vehicles had a market share of 5.4%; hence, 94.6% of newly registered passenger cars still (at least partially) rely on an ICE as the method of propulsion.

In addition to new vehicle sales, there is further potential in reducing carbon emission through alternative fuels [14–19] for existing vehicle fleets. Accordingly, further development of more environmentally friendly ICE technologies is necessary. Monitoring and analyzing engine oil conditions play an essential role in this area, as alternative fuels can influence lubricant degradation [20–23], which could also affect the service life.

The degradation of engine oils during their service life is a well-studied topic [24–34]. The main contributing factors are:

- Accumulation of contaminants, such as soot, water, or fuel,
- Oxidation and nitration through thermo-oxidative degradation and
- Additive depletion, e.g., antioxidant (AO) and antiwear (AW) additive reduction.

Oil condition monitoring is generally carried out by the determination of various chemical parameters, such as total acid number (TAN) and total base number (TBN) [35], oxidation, nitration, and sulfation via Fourier-transformed infrared spectrometry (FTIR) [24,28], a viscosity [28], or analysis of the additive degradation on a molecular level via mass spectrometry [24,36].

The antiwear additive zinc dialkyl dithiophosphate (ZDDP) has been the focus of researchers for many years due to its widespread utilization. Barnes et al. highlighted that wear could either increase or decrease during ZDDP degradation, depending on the degradation mechanism [37]. Cen et al. reported a decrease in wear after artificially altering a ZDDP-containing model lubricant [38], while Agocs et al. reported an increase in wear due to ZDDP depletion during a large-scale artificial alteration of an engine oil [31]. Dörr et al. found that wear initially decreases due to the activation of the ZDDP while later increases, as increasing amounts of inorganic ZDDP degradation products, namely sulphuric acid and phosphoric acid, are formed [36].

Analysis of the tribofilms formed by degraded lubricants is also fairly common. Fuller et al. investigated the interplay of tribofilm chemistry and ZDDP degradation [39] and found a decrease in polyphosphate chain length with the propagation of thermal decomposition. Uy et al. highlighted dissimilarities in the tribofilms formed by aged oil samples [40]. They found less carbonate in films formed by altered oils and showed that only the fresh oil samples formed tribofilms containing sulfides. Dörr et al. also noted that the relative amount of sulfides decreases in the tribofilm due to the alteration of the engine oil [36].

Multivariate data analysis methods, such as principal component analysis (PCA), condense large multi-dimensional datasets by identifying key properties and influences on the data. Additional modeling-based approaches can help in establishing fast diagnostic systems and optimized predictive maintenance strategies. Macián et al. [41] established a regression model to predict total acid number (TAN) and total base number (TBN) values of used engine oil samples based on Fourier Transformed Infrared (FT-IR) spectra. In this case, PCA was an intermediary step to reduce each high-resolution IR spectrum to four principal components that can describe more than 99% variance in the dataset. Gracia et al. [42] utilized PCA to study the effect of iron on the oxidation of base oil. PCA was carried out on FT-IR spectra to identify the differences in critical degradation mechanisms in the presence of iron. Wolak et al. [43] developed a set of mathematical models to describe engine oil degradation based on differential FT-IR spectra of used engine oil samples. Bassbasi et al. [44] utilized FT-IR spectroscopy and multivariate data analysis to differentiate adulterated engine oil samples from high-quality ones. PCA was conducted on the FT-IR spectra of 61 oil samples to reduce the dimensionality of the dataset and identify key characteristics. Srata et al. [45] also applied a chemometric approach to engine oil analysis to distinguish high-quality samples from samples contaminated with low-quality oils. Visible-Near-Infrared (VIS-NIR) spectra were collected from 165 samples that were subjected to PCA to visualize groupings in the dataset. Besser et al. [33] compared the aging behavior of engine oils during artificial alteration and aging of the same oils during chassis dynamometer bench tests using PCA. FT-IR data was used to find similarities and differences in oil degradation mechanisms in the lab and the real system.

Fleet studies are also increasingly common in the literature. Wei et al. investigated the degradation of a lubricant in an urban environment via a passenger car fleet and reported that the coefficient of friction or wear scar area showed no significant increase after 5000 km mileage. In contrast, an increase in the total acid number (TAN) and a decrease in the total base number (TBN) were visible [35]. Dörr et al. studied engine oil degradation in a passenger car during a typical oil change interval and found an increase in the neutralization number (NN) and decrease in the TBN linked to engine oil oxidation, as well as the depletion of antioxidants and ZDDP. Most notably, it was shown via high-resolution mass spectrometry that the dialkyl dithiophosphate additives rapidly deplete while forming dialkyl thiophosphates and subsequently dialkyl phosphates. This

degradation of ZDDP was linked to the observed significant increase in engine wear indicated by the iron content of the engine oil [24]. Agocs et al. highlighted differences between engine oil parameters in diesel and petrol vehicles in multiple fleet studies [28,30], most notably in the trends in oxidation, nitration, soot accumulation, ZDDP degradation, and wear.

A shared characteristic of these studies is that they use a wide variety of analytical results, and consequently, the underlying laboratory work is time-consuming and, hence, cost-intensive. To overcome these drawbacks, the study in hand presents a cost-effective, fast analysis method for advanced engine oil diagnostics through vehicle tracking, FT-IR spectroscopy, and principal component analysis (PCA).

2. Materials and Methods

2.1. Field Test and Selected Vehicles

A 6-month-long field test was performed on a passenger car fleet to gain deeper knowledge on the influence of utilization profiles on engine oil degradation. A total of 47 used oil samples were collected from the 12 vehicles during the 6-month-long observation period. The results of the chemical oil analysis of the fleet test are discussed in [28]; thus, a detailed presentation of the methodology, vehicles used, and engine oil are available in the previous work, and only a brief summary of the fleet test methodology is here presented.

The test fleet was comprised of 12 mid-to-executive size premium vehicles selected from the car fleet. The study's main focus was on petrol-fueled powertrains; thus, nine out of 12 vehicles were selected to include a 2.0 L turbocharged spark ignition direct injection (petrol) engine. The remaining three vehicles were equipped with 2.0 L turbocharged compression ignition direct injection (Diesel) engines. Vehicle speed and mileage data were collected through a GPS tracking system. The vehicles were divided into two categories—"short-range" and "long-range"—based on the average trip length and average speed during the utilization. A vehicle was considered short-range when both the average trip length (13.2 km per trip) and average speed (38.5 km/h) matched that of city traffic, based on the data published in [46] and [47], respectively. Oil samples were taken regularly with intervals of 1 month for short-range and 2500 km for long-range vehicles.

Tables 1 and 2 summarize the properties of diesel and short-range petrol vehicles as well as long-range petrol vehicles, respectively. Oil change ODO represents the total mileage of the vehicle at the time of the oil change (i.e., the start of the study) in kilometers. Mileage represents the cumulated distance traveled by the vehicle during the 6-month-long field study in kilometers. Regarding transmission types, MT stands for manual and AT for automatic transmissions. In the case of drivetrains, FWD designates front-wheel drive and AWD all-wheel drive. Chassis type designations are based on ISO 3833:1977 [48], with the following extensions:

SUV-S: standard size suburban utility vehicle

SUV-C: a compact suburban utility vehicle

SW-E: executive size station wagon

Table 1. Properties of diesel and short-range petrol vehicles.

Vehicle	1	2	3	10	11	12
Engine power (kW)	130	140	140	155	155	155
Engine type	Diesel	Diesel	Diesel	Petrol	Petrol	Petrol
Transmission	MT	AT	AT	AT	AT	AT
Drivetrain	AWD	AWD	FWD	AWD	AWD	FWD
Model year	2014	2017	2016	2013	2012	2011
Curb weight (kg)	1755	1770	1660	1565	1565	1565

Table 1. *Cont.*

Vehicle	1	2	3	10	11	12
Chassis type	SUV-S	SUV-S	E	SUV-C	SUV-C	SUV-C
Oil change ODO (km)	120,122	123,567	71,025	62,745	48,354	106,838
Mileage (km)	12,700	11,700	1300	1700	1100	1800
Range	Long	Long	Long	Short	Short	Short

Table 2. Properties of long-range petrol vehicles.

Vehicle	5	6	7	4	8	9
Engine power (kW)	185	185	185	221	221	221
Engine type	Petrol	Petrol	Petrol	Petrol	Petrol	Petrol
Transmission	AT	AT	AT	AT	AT	AT
Drivetrain	AWD	AWD	AWD	AWD	AWD	AWD
Model year	2018	2018	2018	2014	2014	2016
Curb weight (kg)	1725	1725	1725	1620	1445	1450
Chassis type	SW-E	SW-E	SW-E	C	C	C
Oil change ODO (km)	65,842	63,384	68,171	69,102	73,341	73,726
Mileage (km)	14,700	17,100	9200	8000	5100	7500
Range	Long	Long	Long	Long	Long	Long

2.2. Oil Condition Monitoring

The field study commenced with an oil change; all participating vehicles were filled with fully synthetic engine oil (SAE 0W-30). For the study at hand, only the FT-IR spectra and the associated calculated parameters are considered. The spectra were taken by a Tensor 27 spectrometer (Bruker, Ettlingen, Germany), averaged from 32 transmission scans at the resolution of 2 cm^{-1} (both background and sample). The evaluated parameters consist of:

- Oxidation and nitration using an in-house method described in detail in [24,28,29],
- Sulfation according to ASTM E2412 [49]
- Residual amounts of additives, namely phenolic and aminic antioxidant as well as ZDDP antiwear additive also by an in-house method [24,28,29],
- Soot loading according to ASTM E 2412 [49]
- Water content according to ASTM E 2412 [49]
- Petrol fuel content according to ASTM E 2412 [49]
- Diesel fuel content according to ASTM E 2412 [49]

Table 3 summarizes the applied evaluation methods as well as the respective wavenumbers. Spectra of used samples were compared to the spectra of the fresh oil.

Table 3. Summary of the applied FT-IR evaluation methods.

Parameter	Wavenumber (1/cm)	Measured Spectral Characteristics	Reporting
Phenol AO.	3650	Peak height	Comparative to the fresh oil
Soot	2000	Peak height	Absorption/cm
Oxidation	1720	Peak height	Absorption/cm
Nitration	1630	Peak height	Absorption/cm
Amin AO.	1515	Peak height	Comparative to the fresh oil

Table 3. Cont.

Parameter	Wavenumber (1/cm)	Measured Spectral Characteristics	Reporting
Sulfation	1150	Peak height	Absorption/cm
ZDDP	1020–920	Maximum peak height in range	Comparative to the fresh oil
Water	3500–3150	Area	Absorption/cm
Petrol	755–745	Area	Absorption/cm
Diesel	817–804	Area	Absorption/cm

2.3. Multivariate Data Analysis

Principal component analysis (PCA) is an explorative data analysis method, which breaks down complex relationships in a data matrix to a simpler form. For example, a large number of different samples from various aging conditions can be examined, and trends visualized [33]. PCA's purpose is dimensionality reduction with as little information loss as possible. In PCA, a new orthogonal coordinate system composed of latent variables is calculated. These latent variables u are defined as

$$u = b_1x_1 + b_2x_2 + \dots + b_mx_m$$

u —value of the latent variable, also called score;

x_i —value of the variable;

b_i —value of the loading representing the significance of the respective variable on the model;

m —number of the variables i .

Latent variables, also called principal components (PCs), are a linear combination of the original variables, where the first PC (PC1) represents the direction of the greatest variance in the data. The original data is transformed to the new coordinate system, resulting in so-called scores. Hence, a score plot shows the objects (in this case, the different oil samples) mapped in the new coordinate system, where certain similarities or differences of the objects can be deduced according to the position of the points, i.e., the distances between each other. The so-called loadings, depicted in a loading plot, describe the share of the respective variable values in the total variance of the original data and can be interpreted as the weights for each original variable when computing the PCs. For both score and loading plots, any PCs can be plotted against each other, but it is acceptable to consider PC1 and PC2 only if they explain a sufficiently large proportion of the total variance together [50,51]. Data preprocessing was carried out using Microsoft Excel and Notepad++. The calculation for the PCA was carried out in a self-developed Python 3.8 script using the Singular Value Decomposition-based PCA method of the scikit-learn 0.23.2 package. Visualization was also performed in Python 3.8 using Plotly 4.11.0. A total of 48 observations (47 used oil samples and one fresh oil sample) were analyzed. An FT-IR spectrum with a horizontal resolution of two wavenumbers corresponds to each observation, resulting in 1657 features per observation. Hence, the analyzed dataset comprises 79,536 individual data points.

The objects, i.e., oil samples, were divided into four different categories based on the available information: Engine type (petrol and diesel), engine power (in kW), mileage (in km), and utilization (short-range and long-range). The fresh oil is marked with "fresh oil" or "0".

Two regions of total absorption, i.e., spectral ranges corresponding to the C–C and C–H bonds, were removed, and all remaining wavenumbers were used for the analysis. No further manipulation of the FT-IR spectra was performed, e.g., no baseline correction, as this would remove information regarding the soot loading from the dataset. FT-IR spectra

were centered around 0 but not scaled to a standard deviation of 1 since all investigated values scatter in the same range.

3. Results and Discussion

3.1. Summary of the Chemical Parameters

A detailed analysis of the changes in oil chemistry depending on different fueling and utilization is presented in [28]. For a better overview, some of the most important findings are briefly summarized below.

Figure 1a displays the propagation of oxidation during the field test. As shown, oxidation propagates faster in petrol vehicles, especially the short-range group compared to the diesel ones. Similarly, the depletion of the ZDDP antiwear additive is faster in petrol vehicles, as shown in Figure 1b. Short-range variants once again exhibit a further accelerated trend. These differences can be attributed to the air-to-fuel ratio (AFR) [28]. A lower AFR generally results in a less “clean” combustion, a higher concentration of chemically active species in the exhaust gas, such as carbon monoxide (CO). This, in turn, results in a faster chemical degradation. Petrol vehicles operate at a significantly lower AFR (near stoichiometric ratio), which explains the faster degradation. Additionally, short-range vehicles, characterized by frequent short trips, have an even lower AFR (rich mixture), as the engine control unit injects excess fuel into the combustion chamber to compensate for condensation on the cold cylinder wall. This results in a further decrease in the AFR and a subsequent acceleration of chemical degradation, and it affects a wide variety of additives; the decrease of boron content is accelerated with decreasing AFR (see Table 4) since the presence of chemically active species accelerates the formation of volatile boric acid [28], which can subsequently be removed through the exhaust gas from the engine oil [28].

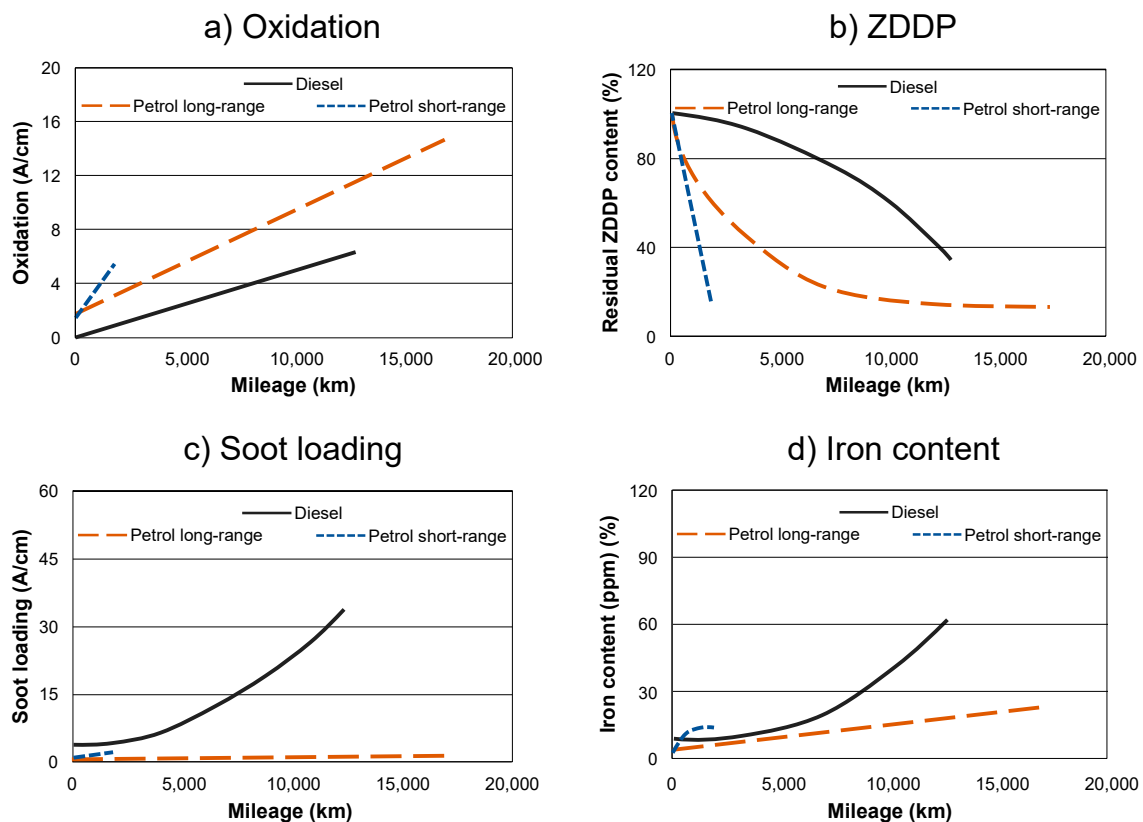


Figure 1. Some observed chemical changes (a) Oxidation; (b) ZDDP depletion; (c) soot loading; (d) iron content (engine wear).

Table 4. Overview of the propagation of various degradation processes.

Parameter	Changes	Diesel Long-Range	Petrol Long-Range	Petrol Short-Range
Oxidation	Increasing			
Nitration	Increasing			
Sulfation	Increasing			
Phenolic antioxidant content	Decreasing			
Aminic antioxidant content	Decreasing			
ZDDP antiwear content	Decreasing			
NN	Increasing			
TBN	Decreasing			
Soot loading	Increasing			
Boron content	Decreasing			
Calcium content	Insignificant	Insignificant changes		
Phosphorus content	Decreasing			
Sulfur content	Decreasing			
Zinc content	Insignificant	Insignificant changes		
Iron content (Engine wear)	Increasing			
Fuel dilution	Increasing			
Kinematic viscosity	Decreasing	Insignificant changes		

Soot accumulates faster in diesel vehicles, as displayed in Figure 1c. This is due to the higher boiling range of the diesel fuel, which results in a lower homogeneity of the mixture, especially when a direct injection is applied. Soot then originates from local fuel-rich regions during the combustion [28]. Figure 1d shows the iron content of the engine oils, which is an indicator of engine wear. Wear processes are complex, but generally, the two main contributing factors are the loss of surface protection (degradation of antiwear additives) and abrasion by particles and soot. The resulting wear is a superposition of the two factors, where diesel vehicles displayed a considerably worse wear performance during the field test.

The chemical characterization of the oil samples revealed that oxidation, nitration, antioxidant and ZDDP antiwear depletion, NN accumulation and TBN reduction, and boron and sulphury depletion were all faster in the case of long-range petrol vehicles than in diesel vehicles which showed a significantly higher soot loading and higher iron content, indicating the engine wear.

Short-range petrol vehicles displayed even faster oxidation, antioxidant, antiwear depletion, TBN reduction, and boron and sulfur depletion. Furthermore, a significant decrease in kinematic viscosity was observed in the case of short-range petrol vehicles, which could directly be attributed to fuel dilution [28]. Table 4 summarizes the differences in the measured parameters. The respective speed of the changes is indicated by the length of the bars and a color code as well, where green corresponds to a slower, yellow to a moderate, and red to a fast degradation process.

3.2. Principal Component Analysis (PCA)—All Vehicles

For the PCA, only the FTIR spectra were considered. This approach is deemed suitable since various oil condition parameters, such as oxidation, nitration, the residual content of multiple oil additives, or soot loading, can be derived directly from said spectra. Moreover, additional oil condition parameters, such as NN and TBN, show collinearity with oxidation [28] or iron content with both residual ZDDP content and soot loading [28], so this information is indirectly contained in the FTIR spectra as well. Since hydrocarbons are the main component of any engine oil, the corresponding spectral ranges are at total absorption, hence contain no information. Accordingly, the corresponding ranges were not considered for the PCA analysis. Figure 2 shows exemplary FTIR spectra of the fresh engine oil as well as a used petrol and diesel sample. Significant absorption peaks are labeled accordingly.

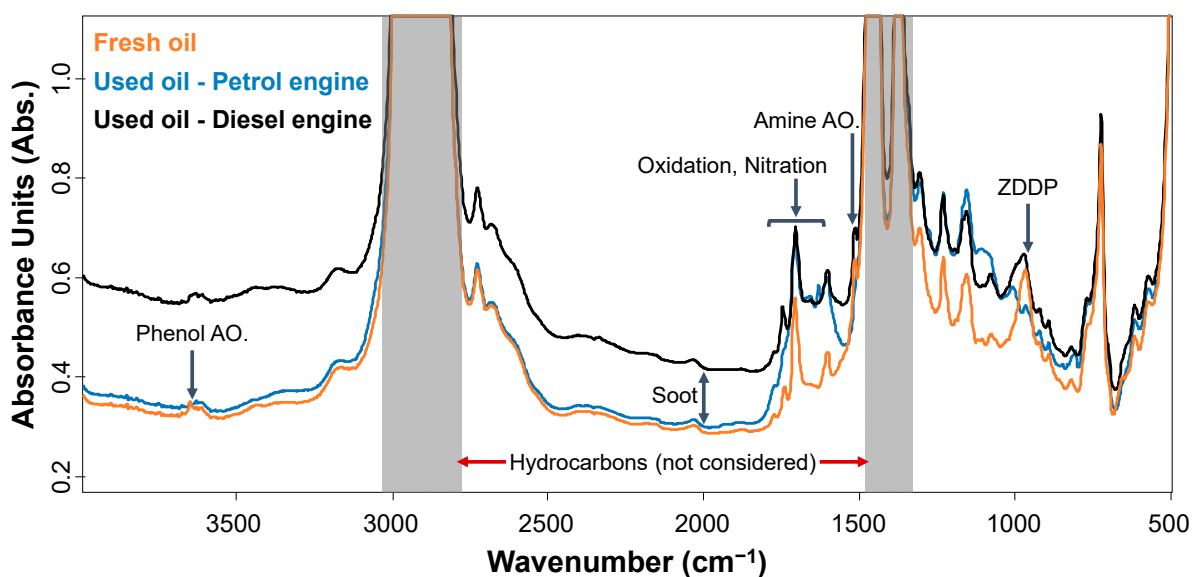


Figure 2. Exemplary FTIR spectra of the fresh engine oil and used petrol and diesel engine oil sample. Significant characteristic absorption peaks are marked for easier visualization.

Figure 3a–d show the PCA score plot of PC1/PC2 of the FTIR spectra, with the objects (oil samples) colored according to different categories. PC1 and PC2 together explain over 99% of the variance in the data, so these two main components are sufficient for data interpretation. In score plot a, where objects are colored according to fuel, a grouping of the petrol engine oil samples can be seen, while the diesel engine oil samples along PC1 are clearly separated from this grouping and form a separate group.

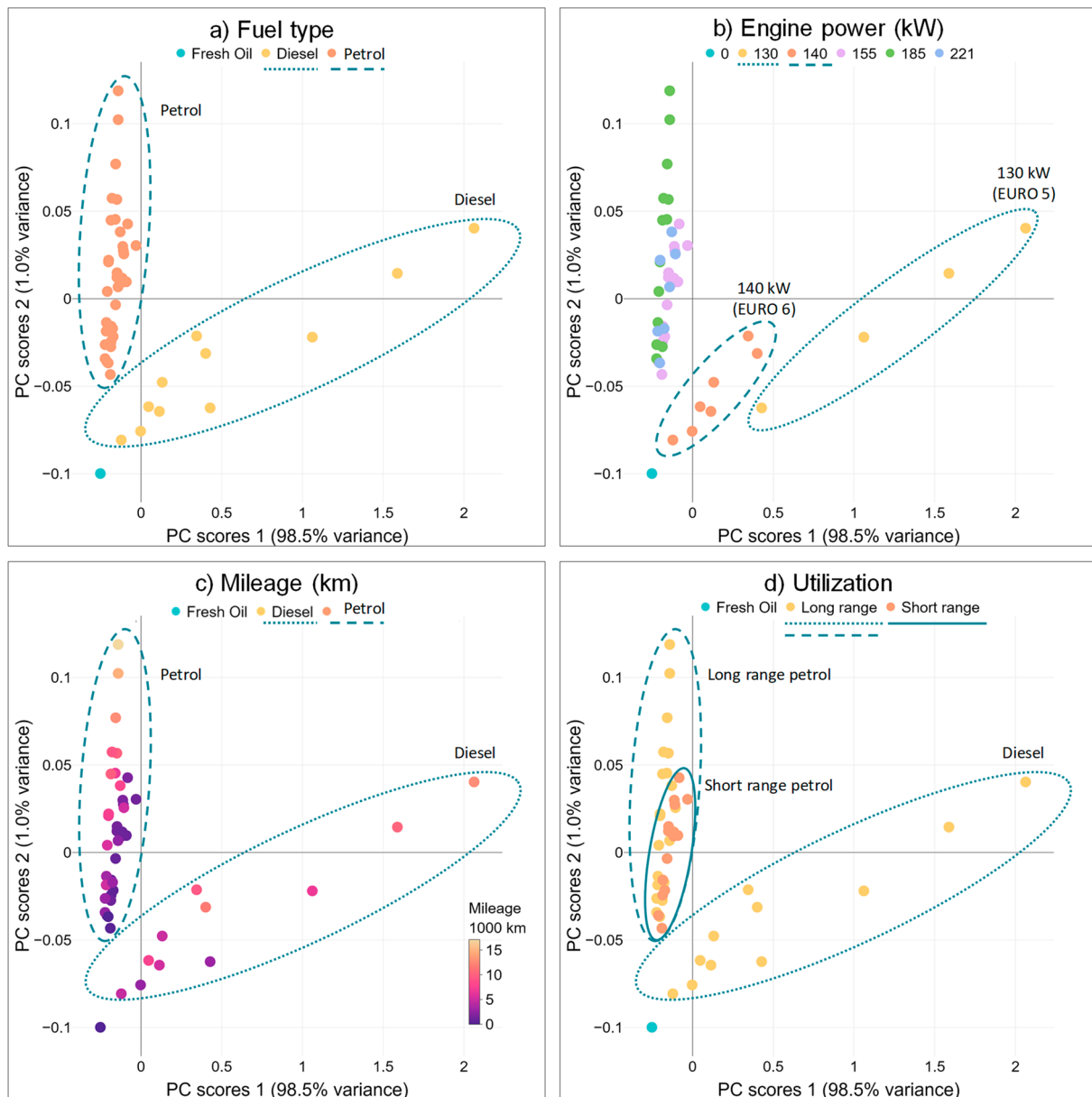


Figure 3. Score–score plots of the FTIR spectra of all vehicles showing PC1 and PC2, objects are colored by: (a) fuel, (b) engine power, (c) mileage, (d) utilization.

When looking at score plot b, where objects are colored according to engine power categories, the 130 and 140 kW diesel vehicles show a clear grouping. Since the displacement and utilization profile of the two is very similar, the separation of the two groups is likely caused by the different engine variant. The 130 kW diesel vehicle was equipped with a slightly older, Euro 5 variant of the 2-liter diesel engine, whereas the 140 kW variant is conformed to Euro 6. Euro 6 diesel engines use a urea-solution to reduce NO_x in the exhausts; hence, they do not rely on higher EGR rates alone to achieve the desired NO_x emission. Furthermore, the 130 kW diesel vehicle included a manual transmission gearbox, while both 140 kW variants have automatic transmissions. An automatic transmission vehicle operates in a narrower engine speed range regardless of the driver, while, in a manual transmission vehicle, the operation range of the engine is dependent on the driver's behavior. This can lead to the 130 kW vehicle being operated more often in an RPM range, which is associated with high EGR, resulting in higher particle mass in the exhaust gas and higher soot loading in the engine oil. The resulting elevated soot loading can be linked

to an increased wear rate, presented in Figure 4, through the iron content of the collected engine oil samples (data from [28]). This indicates that relatively small differences in the engine and drivetrain construction might have a significant impact on the oil degradation and the resulting tribological performance.

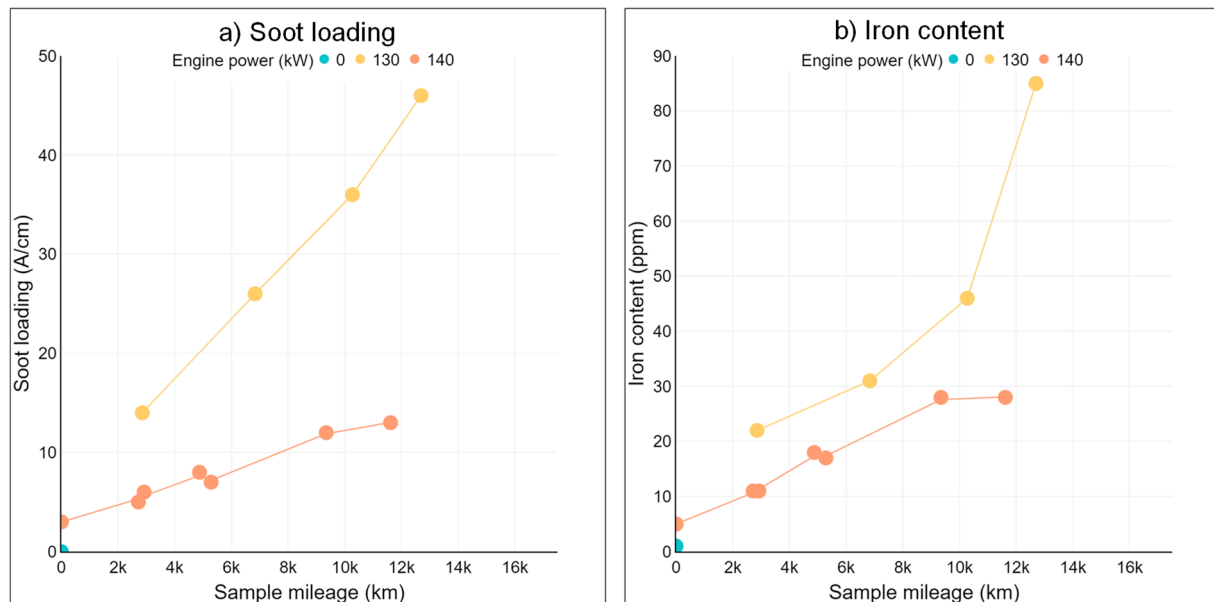


Figure 4. (a) Trends of soot loading of diesel samples plotted against mileage; (b) Trends of the iron content of diesel samples plotted against mileage.

To further analyze the possible effect of vehicle usage, a statistical analysis of the utilization profile indicators (average trip length and average speed) was conducted according to the method described in [30]. This approach was selected instead of PCA due to the limited size of the two groups. First, an F-test was performed to determine whether the variances of the two samples were equal. Then, a Student's *t*-test was carried out, either assuming equal or unequal variances depending on the outcome of the initial F-test (all statistical tests were one-tailed at a significance level of 5%). Student's *t*-test can be used to determine whether the means of two populations are significantly different from each other at a given significance level. It was determined that in the case of the 130 kW and 140 kW diesel engines, neither the average speed nor the average trip length differs significantly when comparing the two populations. Comparatively, in the case of the long-range and short-range petrol vehicles, both indicators show a statistically significant difference. Table 5 displays performed test types and the associated T and critical T values. Accordingly, in the diesel engines, the observed differences between the 130 kW and 140 kW variants are caused by the differences in exhaust aftertreatment technology and transmission type, not due to differences in the utilization profile. However, no similar strong separation based solely on engine power can be observed between long-range vehicles with 185 kW and 221 kW engines as they are all corresponding to the same Euro-class (Euro 6).

Table 5. Performed statistical tests and respective results.

Population 1.	Population 2	Parameter	Test Type	T Value	Critical T Value (One-Tail)	Means Different?
Diesel 130 kW	Diesel 140 kW	Average trip length (km)	Equal variances	11.635	1.729	No
		Average speed (km/h)	Unequal variances	18.827	1.725	No
Petrol 155 kW (short range)	Petrol 185 kW and 221 kW (long range)	Average trip length (km)	Unequal variances	−0.582	1.833	Yes
		Average speed (km/h)	Unequal variances	−1.653	1.860	Yes

In the score plot in Figure 3c, the objects are colored according to the mileage. A tendency can be seen where the oil samples are arranged from bottom to top along PC2 for petrol engines and PC1 and PC2 for diesel engines according to increasing mileage.

In the score plot displayed in Figure 3d, the objects are colored according to the utilization profile, a clear distinction between short-range and long-range petrol engines can be made (detailed analysis see Section 3.3), which corresponds to the findings of the conventional oil analysis in our previous work [28] regarding significant differences due to the different utilization profile. Since the short-range group corresponds to the 155 kW engine group, some differences in the oil condition might emerge due to the dissimilarities in engine construction, but the short-range utilization of all 155 kW vehicles most likely plays a significant role. As displayed in Table 5, the short-range and long-range groups display vastly different average speed and average trip length; thus, it can be assumed that in the case of the petrol engines, both the differences in engine power as well as in the utilization profile are responsible for the different oil condition.

Figure 5 shows the corresponding loading plots of the PCA. Loadings can be considered as “weights”, describing the contribution of a variable (wavenumber) to the position of an object (oil sample) in the score–score plots (see Figure 3). Since the classical loading–loading plot (Figure 5a) can be challenging to interpret, the individual loadings of PC1 and PC2 are also displayed as a function of the wavenumber in Figure 5b and Figure 5c, respectively. When comparing the loadings with the original FTIR spectra, the corresponding chemical structures become evident (see Figure 2). PC1 is mainly influenced by the soot loading (the baseline shift of the spectra caused by particles absorbing equally at all wavelengths [49]); hence, the clear separation of petrol and diesel engine oil samples along PC1 is caused by the significant differences in the soot loading. This is also true for the distribution of the diesel engine oil samples along PC1, as soot is a combustion byproduct [28], and its concentration is proportional to the utilization of the engine. Compared with diesel engine oils, petrol engine oil samples show practically no separation along PC1 since their soot loading is marginal. The short-range petrol vehicles display a minor separation along PC1, which corresponds well with the findings of the previous studies [28], where the slightly higher soot loading was found.

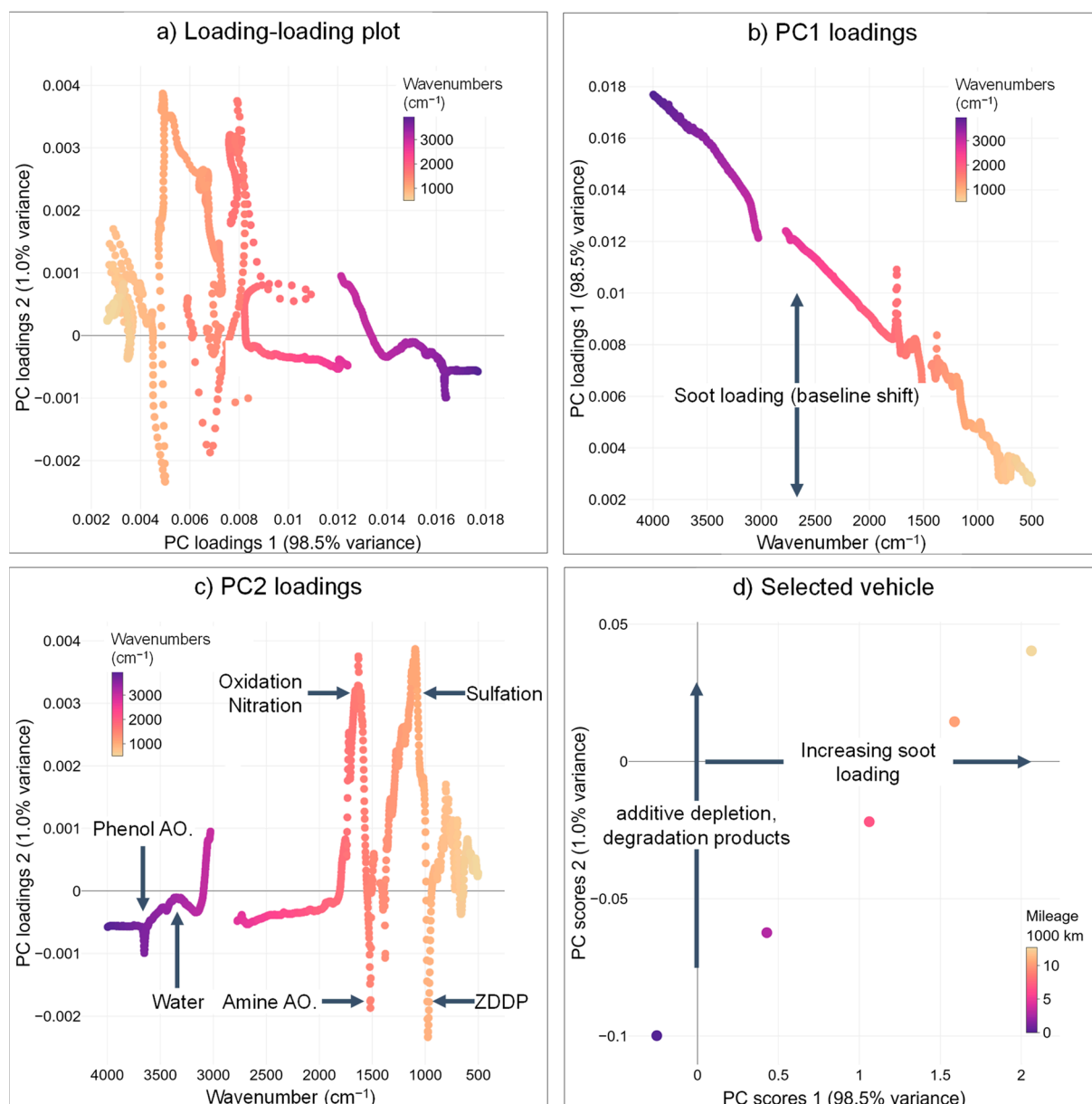


Figure 5. Loadings of the FTIR spectra of all vehicles. (a) Loading-loading plot, (b) PC1 loadings, (c) PC2 loadings, (d) Score–score plot of a selected 130 kW diesel vehicle. Loading plots: objects are colored according to wavenumbers. Score plot: objects are colored according to mileage.

Main contributors to PC2 are the depleting engine oil additives, e.g., phenolic antioxidants and ZDDP, as well as the emerging degradation products, e.g., from oxidation and nitration. Considering the score–score plots, it is visible that the samples separate along PC2 with increasing utilization, hence, increasing changes in residual additive contents and amount of degradation products. Additionally, petrol engine oil samples show a greater separation along PC2 compared with the diesel engine oils, which corresponds to the more pronounced additive depletion and higher concentration of degradation products seen on many occasions in the previous studies [28]. For better visualization of the mentioned effects, the oil samples of a single vehicle (130 kW diesel) are shown in Figure 5d, where the objects are colored according to the sample mileage. When considering a single vehicle, it is clearly visible how the changes in soot loading and residual additive content and degradation product concentration cause the separation along PC1 and PC2, respectively.

3.3. Principal Component Analysis (PCA)—Petrol Vehicles Only

A further interesting aspect is the explained variance of the displayed PCs. PC1 explains 98.5% of the total variance in the data while PC2 only 1% in total when considering all vehicles, as displayed in Figure 3a–d. PC1 directly corresponds to soot loading, which is one of the main differences between petrol and diesel vehicles. Since the very high variance of PC1 has a substantial influence on the analysis and might “mask” some minor differences, a second PCA was carried out, which excluded all diesel samples. Figure 6 depicts the scores of petrol samples from the second principal component analysis. To further accentuate the effect of utilization on engine oil degradation, two additional usage parameters were introduced—the number of cold starts calculated based on the number of trips taken by each vehicle and the interquartile range of speed. The number of cold starts was determined by counting the number of trips where at least 60 min had passed between two adjacent cruises. As most of the fleet study happened during the fall of 2019 in cold weather, it is reasonable to assume that 60 min of downtime was enough for the lubricant to cool under the ideal 90 °C–100 °C operating temperature range.

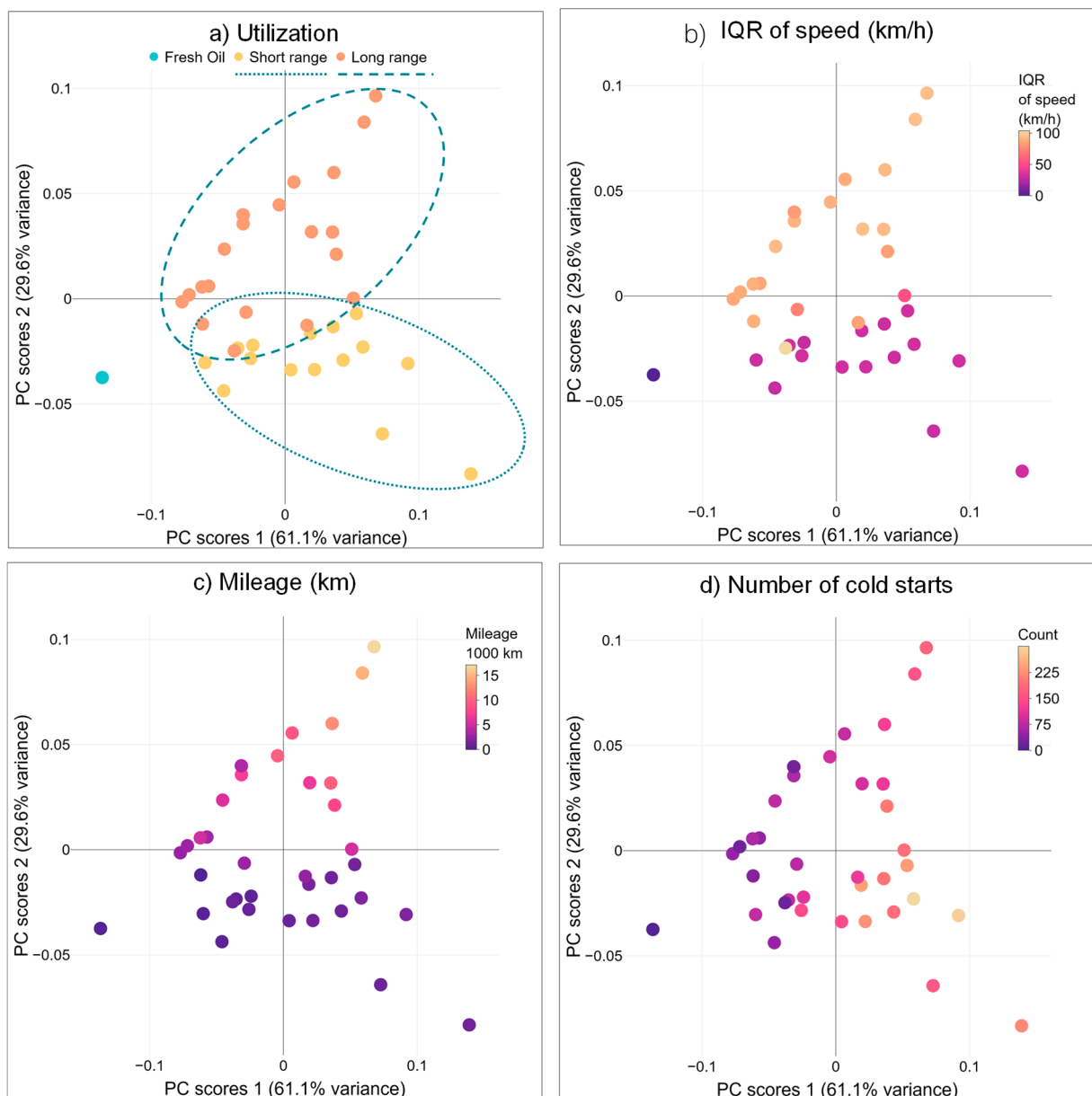


Figure 6. Score–score plots of the FTIR spectra of the petrol vehicles, showing PC1 and PC2, objects are colored by: (a) number of cold starts, (b) IQR of speed, (c) mileage, (d) utilization.

The interquartile range (IQR) is a statistic property of a dataset, which describes the distance between the first (Q1) and third (Q3) quartile. Quartiles divide the dataset into four equal parts, where Q1 corresponds to the lower 25%, and Q3 corresponds to the upper 25%.

The score plot presents objects scattered in two directions starting from the reference sample (fresh oil). Coloring the objects by utilization reveals a clear separation of short-range and long-range vehicles, as already discussed in Section 3.2 (Figure 6a). In addition, coloring objects by the IQR of speed during the sampling period presents an identical grouping of predominantly low speed (short-range, <30 km/h IQR) and moderate-to-high speed (long-range, 50–100 km/h IQR) cars (Figure 6b). Comparing these groupings with mileage readings (Figure 6c) and the number of cold starts (Figure 6d) further underlines the disparity between the investigated use scenarios. Higher mileages were achieved by long-range vehicles, which presents a shift towards the upper-right region of the score plot. In contrast, short-range vehicles endured numerous cold starts, which contributed to a shift towards the lower right region.

Considering these observations based on the PCA of petrol engine samples, PC1 in Figure 6 can be intuitively correlated with the number of cold starts, whereas PC2 is proportional to the length of individual trips, as frequent long trips sum up to higher overall mileage.

An analysis of the loadings for the petrol samples (Figure 7a,b) reveals a more nuanced contribution of variables to the position of each object compared to the previous PCA. No baseline shift is visible in this case due to the insignificant amount of soot in petrol samples. The main influencing factors are the depletion of additives, oxidation, nitration, and sulfation, as well as the accumulation of water and petrol fuel. (See Table 3 for the respective wavenumbers).

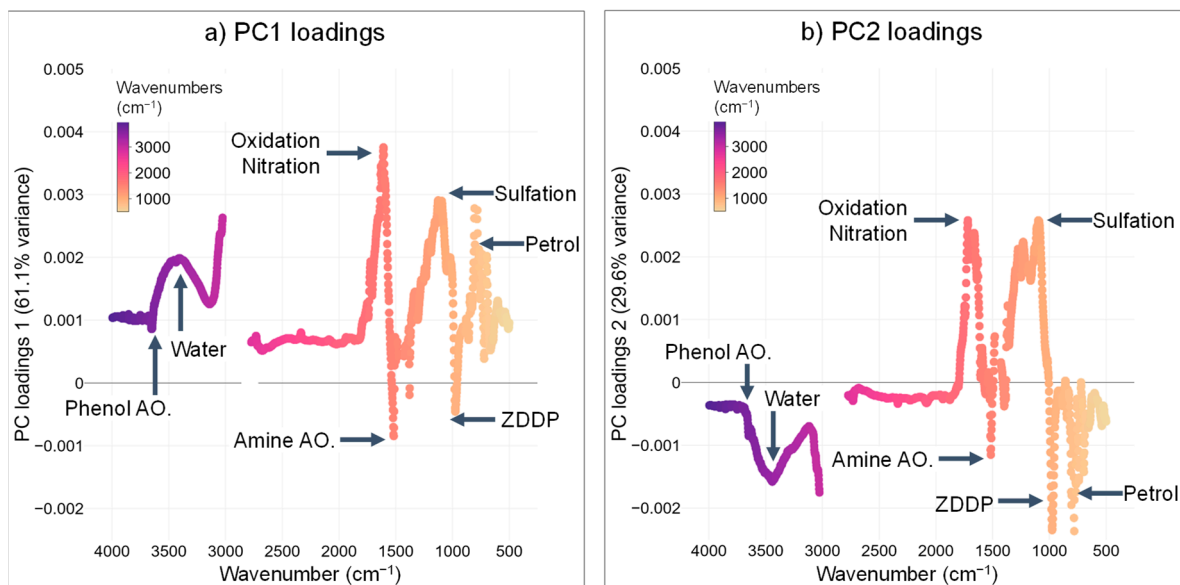


Figure 7. Loadings of the FTIR spectra of the petrol vehicles. (a) PC1 loadings, (b) PC2 loadings. Loading plots: objects are colored according to wavenumbers.

As both PCs contain indicators of oil degradation, an interpretation is less trivial. To achieve a comprehensive overview, a correlation with additional oil parameters is taken into account. A drop in engine oil viscosity resulting from the regular operation is a consequence of fuel dilution and aggregation of water in the lubricant. Detailed fuel dilution data of selected samples was published in the previous study [28], which indicated a dilution level of 3.65 m% for a petrol vehicle after short-range operation for 1750 km. A consequent viscosity drop of 25.4% in the case of the short-range petrol vehicle was

experienced. To validate the correlation of fuel dilution and the decrease in viscosity, a sample of fresh oil was mixed with 3.65 m% petrol, which yielded a measured viscosity change of -26.8% . In comparison, a separate petrol-operated long-range passenger car showed only 0.55 m% fuel dilution and 3.9% viscosity change after 17,100 km mileage.

Oxidation and NN generally display a linear relationship, as shown in Figure 8a. This is expected, as the organic acids responsible for the increase in the NN are oxidation products [28,29]. Comparatively, the TBN on Figure 8b also shows a close relationship with the NN (and subsequently with the oxidation), as the depletion of the base reserve is caused by the acidification of the engine oil matrix and the subsequent neutralization reactions [28].

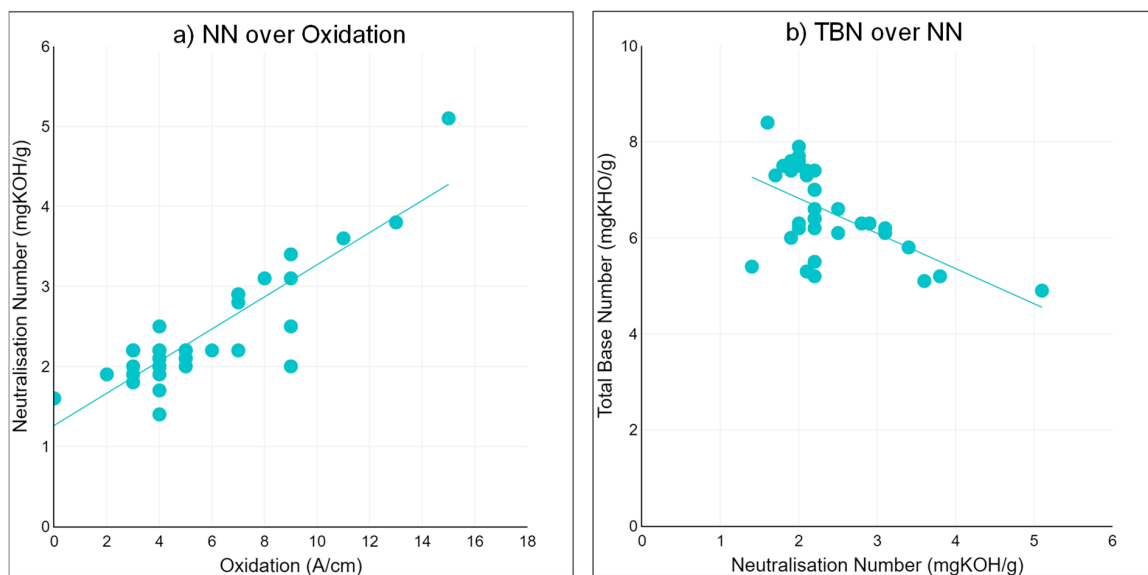


Figure 8. Relationship between the oxidation and NN (a) as well as NN and TBN (b).

Correlating the loading and score plots sheds light on the relationship between usage characteristics and oil degradation attributes. Figure 9 presents the score–score plot with objects colored by quantified engine oil properties from the previous study.

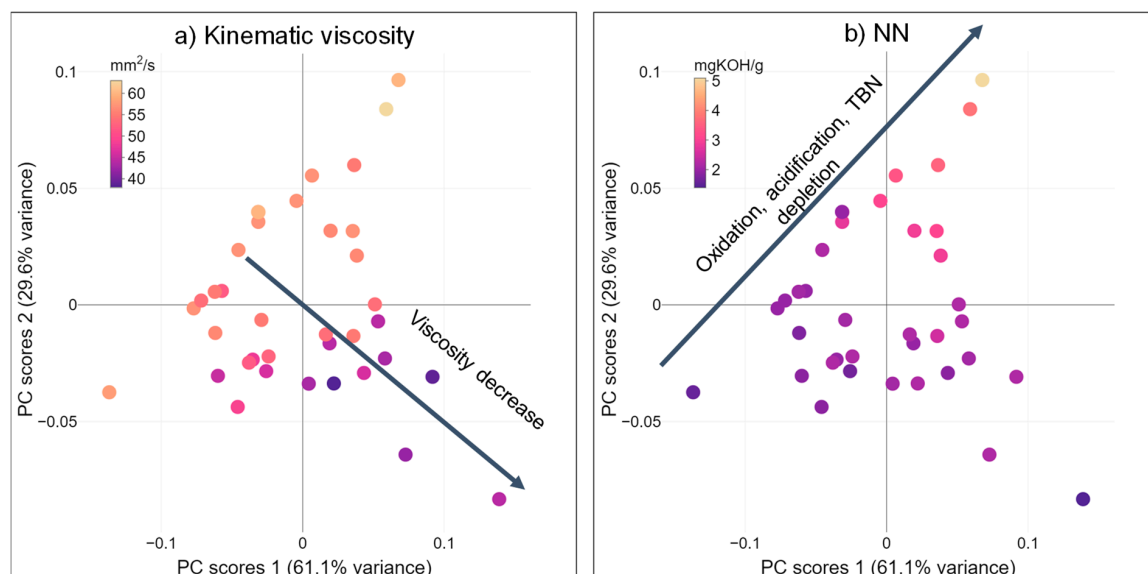


Figure 9. Score–score plots of the FTIR spectra of the petrol vehicles, showing PC1 and PC2 with an interpretation of the observed scattering, objects are colored by: (a) kinematic viscosity, (b) neutralization number.

Short-range utilization, along with an increased number of cold starts (frequent short trips), has a pronounced effect on water and fuel content, as these species cannot effectively evaporate on a lower operating temperature, which is prevalent in this case (separation along PC2). One indicator of this is the observed decrease in the kinematic viscosity amongst others (Figure 9a). Accordingly, the separation of the short- and long-range populations is essentially the lower operating temperature of the short-range vehicles, which results in the accumulation of “light” species.

Figure 9b shows objects colored by neutralization number, which provides evidence that long-range utilization and increased mileage (frequent long trips) contribute to increased oxidation, subsequent NN increase, and TBN depletion, as these vehicles reach a higher total mileage and a higher degree of oil degradation.

Furthermore, the ability to reliably correlate observed separation in the FT-IR spectra-based PCA and “independent” oil parameters, such as NN, TBN, and viscosity, shows the robustness of the applied data analysis method. Nevertheless, a comprehensive understanding of oil degradation and its underlying physicochemical changes is needed for a correct interpretation.

4. Merits of the PCA Approach

The interpretation of FT-IR spectra—although partially standardized—is not trivial. For example, spectral interferences of contaminants or oil additives might present a challenge. Even the calculation of oxidation, one of the most common oil condition parameters, is rather complex, utilizing a conventional approach. e.g., ASTM E2412 accepts the area between 1800 cm^{-1} and 1670 cm^{-1} as a general value, or between 1710 cm^{-1} and 1660 cm^{-1} for ester-based oils due to the interference of the carbonyl peak of the base oil. Alternatively, the absorbance of the peak closest to 1709 cm^{-1} can be considered as well [44]. The selection of the proper method requires the identification of the present peaks and knowledge of the underlying chemistry. In fact, ASTM states the following in [49]: “Different laboratories have developed slight variation on these analyses. These different approaches are equally valid for trending, but will produce results that differ numerically. Consistent analyses should be applied for each application.” Accordingly, not even the corresponding standards offer clear guidance regarding integration ranges. This makes the application of FT-IR results by on-site personal such as machine operators problematic.

The presented method utilizing PCA takes the raw FT-IR spectra; therefore, knowledge of the conventional interpretation of FT-IR results is not necessarily required. This is helpful for the end user since the approach can be used to automatically compare an oil sample to a reference database containing acceptable and problematic oil samples. Subsequently, a decision can be made by on-site technical personnel as to whether an oil change is necessary, solely based on the position of the sample on the score–score plot, without any training on oil chemistry or FT-IR evaluation methods. Furthermore, when a sufficient reference database is available, models can be simplified by selecting only the most suitable reference samples, e.g., vehicles with the same fueling or exhaust aftertreatment for any individual scenario.

Although the correct interpretation of the PCA loading plots that explains why an oil sample has its respective position is not trivial, it is noteworthy how much information can be derived from a relatively simple, common, and cost-efficient analytical technique, such as FTIR spectrometry when evaluating and interpreting the data according to this method.

Most studies present PCA as an intermediary step in modeling physicochemical behavior [41] or clustering data [45], whereas an insightful analysis of the loadings as presented in Sections 3.2 and 3.3, as well as [23,42] can lead to a deeper understanding of the underlying phenomena as well. PCA coupled with a mathematical modeling approach can be used to develop predictive models for engine oil diagnostics [44] that can help optimize fleet maintenance strategies or identify malicious attempts at adulterating lubricants [45]. An additional benefit of implementing PCA in an open-source software

environment as Python is the easy integration of the analysis method to IT systems already present at the end user.

5. Conclusions

To summarize, several important differences between used petrol and diesel engine oils can be shown when utilizing multivariate data analysis, in this case, principal component analysis (PCA). Accordingly, parameters such as fueling (see Figure 3a), mileage, utilization profile (see Figure 6a), and variations in engine properties, e.g., exhaust aftertreatment (see Figures 3b and 4), all have a significant impact on the oil degradation, hence on the tribological performance of the engine oil as well. It was shown that most of the differences regarding additive depletion or degradation product and soot accumulation can be identified by a single analysis when using multivariate techniques.

Petrol and diesel vehicles separate on the one hand due to the faster chemical degradation of petrol engine oils, which can be attributed to the lower AFR in the case of spark-ignition engines. On the other hand, a further reason for their separation is the soot loading, which is high in the case of the diesel vehicles, due to the higher boiling point of the diesel fuel, which results in local inhomogeneities of the mixture and propagates soot build-up. Analysis of the short-range and long-range petrol vehicles showed that the main reason for separation is the accumulation of water and petrol in the short-range engine oils, which can be attributed to the lower engine temperature and higher number of cold starts, frequent during short-range operation.

The results correspond well with findings regarding differences when considering all engine oil parameters [28]; however, obtaining an overview of all the samples and the emerging differences is a lot simpler. Thus, the PCA presents a user-friendly approach to fleet tracking and oil condition monitoring in case of both condition-based and predictive maintenance strategies. As only simple FT-IR spectra are needed, no further oil analyses, e.g., NN and TBN titrations of water content evaluation, are required. Still, as demonstrated, the “loss of information” is minimal, as most conventional parameters are indirectly contained in the FT-IR spectra.

Author Contributions: Conceptualization: A.L.N. and A.A.; Data curation: A.L.N. and A.A.; Formal analysis: A.L.N., A.A. and B.R.; Funding acquisition: P.R., J.R.-B. and N.D.; Investigation: A.L.N. and A.A.; Methodology: A.L.N. and A.A.; Project administration: A.L.N., C.B. and P.R.; Resources: P.R.; Software: A.L.N. and B.R.; Supervision: J.R.-B. and N.D.; Validation: A.L.N. and A.A.; Visualization: A.L.N. and A.A.; Writing—original draft: A.L.N., A.A. and C.B.; Writing—review & editing: A.L.N., A.A., J.R.-B., P.R., C.B. and N.D. All authors have read and agreed to the published version of the manuscript.

Funding: This work was partly funded by the “Austrian COMET Program” (project InTribology, No. 872176) via the Austrian Research Promotion Agency (FFG) and the Provinces of Niederösterreich and Vorarlberg. Oil characterization and oil data evaluation have been carried out within the “Excellence Centre of Tribology” (AC2T research GmbH).

Institutional Review Board Statement: Not applicable.

Informed Consent Statement: Not applicable.

Data Availability Statement: Restrictions apply to the availability of these data. Data was obtained from AUDI HUNGARIA Zrt. and are available from the authors with the permission of AUDI HUNGARIA Zrt.

Acknowledgments: The authors would like to thank the general support of AUDI HUNGARIA Zrt. in carrying out the field study.

Conflicts of Interest: The authors declare no conflict of interest.

References

1. Commission Launches the Fit for 55% Package. Available online: https://www.interregeurope.eu/policylearning/news/12610/commission-launches-the-fit-for-55-package/?no_cache=1&cHash=a371af17736f1f2f09030ee45e7dd6f2 (accessed on 30 August 2021).
2. Cui, H.; Hall, D.; Lutsey, N. *Update on the Global Transition to Electric Vehicles through 2019*; International Council on Clean Transportation: Beijing, China; Berlin, Germany, 2020. Available online: <https://theicct.org/publications/update-global-ev-transition-2019> (accessed on 30 August 2021).
3. Baldwin, R. Toyota Is Finally Making an Electric Vehicle, Plans More. Available online: <https://www.caranddriver.com/news/a34896309/toyota-electric-cars-plans-revealed/> (accessed on 30 August 2021).
4. Blanco, S. Honda, VW Making Wildly Different Bets on Our Electric Future. Available online: <https://www.caranddriver.com/news/a30350065/honda-vw-electric-cars-future/> (accessed on 30 August 2021).
5. Reuters BMW Aims for 20% of Its Vehicles to Be Electric by 2023 -Paper. Available online: <https://www.reuters.com/article/bmw-electric-idUSKBN2910GV> (accessed on 30 August 2021).
6. Toyota Mirai Breaks World Record for Distance Driven with One Fill of Hydrogen. Available online: <https://newsroom.toyota.eu/toyota-mirai-breaks-world-record-for-distance-driven-with-one-fill-of-hydrogen/> (accessed on 30 August 2021).
7. BMW Starts European Road Tests of Hydrogen Fuel Cell Cars. Available online: <https://www.cnn.com/2021/06/17/bmw-starts-european-road-tests-of-hydrogen-fuel-cell-cars.html> (accessed on 30 August 2021).
8. Volkswagen Investiert in Batterie-Standort Salzgitter. Available online: https://www.volkswagenag.com/de/news/2020/05/Volkswagen_invests_in_battery_operations_at_Salzgitter.html# (accessed on 30 August 2021).
9. “Automotive Cells Company”: Groupe PSA und Total schaffen Joint Venture zur Produktion von Batterien in Europa. Available online: https://media.stellantis.de/de/Automotive-Cells-Company-Groupe-PSA-und-Total-schaffen-Joint-Venture-zur-Produktion-von-Batterien-in-Europa_03092020 (accessed on 30 August 2021).
10. H2—Key Player in the Maritime Energy Transition. Available online: <https://www.man-es.com/marine/strategic-expertise/future-fuels/hydrogen> (accessed on 30 August 2021).
11. Cummins Begins Testing of Hydrogen Fueled Internal Combustion Engine. Available online: <https://www.cummins.com/news/releases/2021/07/13/cummins-begins-testing-hydrogen-fueled-internal-combustion-engine> (accessed on 30 August 2021).
12. Toyota Developing Hydrogen Engine Technologies Through Motorsports. Available online: <https://global.toyota/en/newsroom/corporate/35209996.html> (accessed on 30 August 2021).
13. Fuel Types of New Passenger Cars in the, EU. Available online: <https://www.acea.auto/figure/fuel-types-of-new-passenger-cars-in-eu/> (accessed on 30 August 2021).
14. Qian, Y.; Zhu, L.; Wang, Y.; Lu, X. Recent progress in the development of biofuel 2,5-dimethylfuran. *Renew. Sustain. Energy Rev.* **2015**, *41*, 633–646. [\[CrossRef\]](#)
15. Omari, A.; Heuser, B.; Pischinger, S. Potential of oxymethylenether-diesel blends for ultra-low emission engines. *Fuel* **2017**, *209*, 232–237. [\[CrossRef\]](#)
16. Aakko-Saksa, P.; Koponen, P.; Roslund, P.; Laurikko, J.; Nylund, N.-O.; Karjalainen, P.; Rönkkö, T.; Timonen, H. Comprehensive emission characterisation of exhaust from alternative fuelled cars. *Atmos. Environ.* **2020**, *236*, 117643. [\[CrossRef\]](#)
17. Chen, Y.; Ma, J.; Han, B.; Zhang, P.; Hua, H.; Chen, H.; Su, X. Emissions of automobiles fueled with alternative fuels based on engine technology: A review. *J. Traffic Transp. Eng.* **2018**, *5*, 318–334. [\[CrossRef\]](#)
18. Niethammer, B.; Wodarz, S.; Betz, M.; Haltenort, P.; Oestreich, D.; Hackbarth, K.; Arnold, U.; Otto, T.; Sauer, J. Alternative Liquid Fuels from Renewable Resources. *Chem. Ing. Tech.* **2018**, *90*, 99–112. [\[CrossRef\]](#)
19. Semelsberger, T.A.; Borup, R.L.; Greene, H.L. Dimethyl ether (DME) as an alternative fuel. *J. Power Sources* **2006**, *156*, 497–511. [\[CrossRef\]](#)
20. Costa, H.L.; Spikes, H. Effects of Ethanol Contamination on Friction and Elastohydrodynamic Film Thickness of Engine Oils. *Tribol. Trans.* **2015**, *58*, 158–168. [\[CrossRef\]](#)
21. Nagy, A.L.; Singer, A. The impact of RME biodiesel on base oil aging—A friction and wear study. In Proceedings of the 7th European Conference on Tribology, Vienna, Austria, 12–14 June 2019; pp. 55–56.
22. Nagy, A.L.; Knaup, J.; Zsoldos, I. A friction and wear study of laboratory aged engine oil in the presence of diesel fuel and oxymethylene ether. *Tribol. Mater. Surfaces Interfaces* **2019**, *13*, 20–30. [\[CrossRef\]](#)
23. Nagy, A.L.; Rohde-Brandenburger, J.; Zsoldos, I. Artificial Aging Experiments of Neat and Contaminated Engine Oil Samples. *Lubricants* **2021**, *9*, 63. [\[CrossRef\]](#)
24. Dörr, N.; Agocs, A.; Besser, C.; Ristić, A.; Frauscher, M. Engine Oils in the Field: A Comprehensive Chemical Assessment of Engine Oil Degradation in a Passenger Car. *Tribol. Lett.* **2019**, *67*, 68. [\[CrossRef\]](#)
25. Rudnick, L.R. *Lubricant Additives*, 2nd ed.; CRC Press: Boca Raton, FL, USA, 2017; ISBN 9781315120621.
26. Diaby, M.; Sablier, M.; Le Negrate, A.; El Fassi, M.; Bocquet, J. Understanding carbonaceous deposit formation resulting from engine oil degradation. *Carbon N. Y.* **2009**, *47*, 355–366. [\[CrossRef\]](#)
27. Khuong, L.S.; Zulkifli, N.W.M.; Masjuki, H.H.; Mohamad, E.N.; Arslan, A.; Mosarof, M.H.; Azham, A. A review on the effect of bioethanol dilution on the properties and performance of automotive lubricants in gasoline engines. *RSC Adv.* **2016**, *6*, 66847–66869. [\[CrossRef\]](#)

28. Agocs, A.; Nagy, A.L.; Tabakov, Z.; Perger, J.; Rohde-Brandenburger, J.; Schandl, M.; Besser, C.; Dörr, N. Comprehensive assessment of oil degradation patterns in petrol and diesel engines observed in a field test with passenger cars—Conventional oil analysis and fuel dilution. *Tribol. Int.* **2021**, *161*, 107079. [CrossRef]
29. Besser, C.; Agocs, A.; Ronai, B.; Ristic, A.; Repka, M.; Jankes, E.; McAleese, C.; Dörr, N. Generation of engine oils with defined degree of degradation by means of a large scale artificial alteration method. *Tribol. Int.* **2019**, *132*, 39–49. [CrossRef]
30. Agocs, A.; Budnyk, S.; Frauscher, M.; Ronai, B.; Besser, C.; Dörr, N. Comparing oil condition in diesel and gasoline engines. *Ind. Lubr. Tribol.* **2020**, *72*, 1033–1039. [CrossRef]
31. Agocs, A.; Budnyk, S.; Besser, C.; Ristic, A.; Frauscher, M.; Ronai, B.; Dörr, N. Production of Used Engine Oils with Defined Degree of Degradation in a Large-scale Device: Correlation of Artificially Altered Oils with Field Samples. *Acta Tech. Jaurinensis* **2020**, *13*, 131–150. [CrossRef]
32. Besser, C.; Schneidhofer, C.; Dörr, N.; Novotny-Farkas, F.; Allmaier, G. Investigation of long-term engine oil performance using lab-based artificial ageing illustrated by the impact of ethanol as fuel component. *Tribol. Int.* **2012**, *46*, 174–182. [CrossRef]
33. Besser, C.; Dörr, N.; Novotny-Farkas, F.; Varmuza, K.; Allmaier, G. Comparison of engine oil degradation observed in laboratory alteration and in the engine by chemometric data evaluation. *Tribol. Int.* **2013**, *65*, 37–47. [CrossRef]
34. Besser, C.; Steinschütz, K.; Dörr, N.; Novotny-Farkas, F.; Allmaier, G. Impact of engine oil degradation on wear and corrosion caused by acetic acid evaluated by chassis dynamometer bench tests. *Wear* **2014**, *317*, 64–76. [CrossRef]
35. Wei, L.; Duan, H.; Jin, Y.; Jia, D.; Cheng, B.; Liu, J.; Li, J. Motor oil degradation during urban cycle road tests. *Friction* **2020**, *9*, 1002–1011. [CrossRef]
36. Dörr, N.; Brenner, J.; Ristic, A.; Ronai, B.; Besser, C.; Pejaković, V.; Frauscher, M. Correlation Between Engine Oil Degradation, Tribochemistry, and Tribological Behavior with Focus on ZDDP Deterioration. *Tribol. Lett.* **2019**, *67*. [CrossRef]
37. Barnes, A.M.; Bartle, K.D.; Thibon, V.R.A. A review of zinc dialkyldithiophosphates (ZDDPS): Characterisation and role in the lubricating oil. *Tribol. Int.* **2001**, *34*, 389–395. [CrossRef]
38. Cen, H.; Morina, A.; Neville, A. Effect of lubricant ageing on lubricant physical and chemical properties and tribological performance. Part I: Effect of lubricant chemistry. *Ind. Lubr. Tribol.* **2018**, *70*, 385–392. [CrossRef]
39. Fuller, M.L.S.; Kasrai, M.; Bancroft, G.M.; Fyfe, K.N.; Tan, K.H. Solution decomposition of zinc dialkyl dithiophosphate and its effect on antiwear and thermal film formation studied by X-ray absorption spectroscopy. *Tribol. Int.* **1998**, *31*, 627–644. [CrossRef]
40. Uy, D.; Simko, S.J.; Carter, R.O.; Jensen, R.K.; Gangopadhyay, A.K. Characterization of anti-wear films formed from fresh and aged engine oils. *Wear* **2007**, *263*, 1165–1174. [CrossRef]
41. Macián, V.; Tormos, B.; García-Barberá, A.; Tsolakis, A. Applying chemometric procedures for correlation the FTIR spectroscopy with the new thermometric evaluation of Total Acid Number and Total Basic Number in engine oils. *Chemom. Intell. Lab. Syst.* **2021**, *208*, 104215. [CrossRef]
42. Gracia, N.; Thomas, S.; Bazin, P.; Duponchel, L.; Thibault-Starzyk, F.; Lerasle, O. Combination of mid-infrared spectroscopy and chemometric factorization tools to study the oxidation of lubricating base oils. *Catal. Today* **2010**, *155*, 255–260. [CrossRef]
43. Wolak, A.; Molenda, J.; Zajac, G.; Janocha, P. Identifying and modelling changes in chemical properties of engine oils by use of infrared spectroscopy. *Measurement* **2021**, *186*, 110141. [CrossRef]
44. Bassbasi, M.; Hafid, A.; Platikanov, S.; Tauler, R.; Oussama, A. Study of motor oil adulteration by infrared spectroscopy and chemometrics methods. *Fuel* **2013**, *104*, 798–804. [CrossRef]
45. Srata, L.; Farres, S.; Fethi, F. Engine oil authentication using near infrared spectroscopy and chemometrics methods. *Vib. Spectrosc.* **2019**, *100*, 99–106. [CrossRef]
46. O’Kelly, M.; Niedzielski, M. Efficient spatial interaction: Attainable reductions in metropolitan average trip length. *J. Transp. Geogr.* **2008**, *16*, 313–323. [CrossRef]
47. Studie: Das Verkehrstempo in Großstädten Sinkt. Available online: https://www.focus.de/auto/news/studie-das-verkehrstempo-in-grossstaedten-sinkt-duesseldorfer-fahren-am-langsamsten_id_11269331.html (accessed on 14 September 2021).
48. ISO 3833:1977 Road Vehicles—Types—Terms and Definitions; International Organization for Standardization: Geneva, Switzerland, 1977.
49. ASTM E2412-10(2018). *Standard Practice for Condition Monitoring of In-Service Lubricants by Trend Analysis Using Fourier Transform Infrared (FT-IR) Spectrometry*; ASTM International: West Conshohocken, PA, USA, 2018.
50. Varmuza, K.; Filzmoser, P. *Introduction to Multivariate Statistical Analysis in Chemometrics*, 1st ed.; CRC Press: Boca Raton, FL, USA, 2016; ISBN 9780429145049.
51. Brereton, R.G. *Chemometrics*; John Wiley & Sons, Ltd.: Chichester, UK, 2003; ISBN 0471489778.